EUROPEAN ORGANIZATION FOR NUCLEAR RESEARCH

Proposal to the ISOLDE and Neutron Time-of-Flight Committee

Implantation of ^{226}Ra for the measurement of its absolute nuclear charge radius

April 9, 2024

S. Bara[1], T.E. Cocolios[1], M. Deseyn[1], Ch.E. Düllmann[2,3,4], A. Doinaki[5,6], C. Duchemin[7], M. Heines[1], J.D. Johnson[1], A. Knecht[5], R. Mancheva[1,7], E. Maugeri[5], W.W.M.M. Phyo[1], P. Reiter[8], D. Renisch[2,4], N. Ritjoho[9], J. Schell[10], J. Shaw[1], K. von Schoeler[6], S.M. Vogiatzi[1], W. Wojtaczka[1], A. Zendour[5]
for the muX collaboration

[1]*KU Leuven, Belgium*
[2]*Johannes Gutenberg University Mainz, Germany*
[3]*GSI Helmholtzzentrum für Schwerionenforschung Darmstadt, Germany*
[4]*Helmholtz Institute Mainz, Germany*
[5]*Paul Scherrer Institut, Villigen, Switzerland*
[6]*ETH Zürich, Switzerland*
[7]*CERN, Switzerland*
[8]*Universität zu Köln, Germany*
[9]*Suranaree University of Technology, Nakhon Ratchasima, Thailand*
[10]*CENIDE, Essen, Germany*

Spokesperson: T.E. Cocolios [thomas.elias.cocolios@cern.ch]
A. Knecht [a.knecht@psi.ch]
Contact person: M. Kowalska [magdalena.kowalska@cern.ch]

CERN-INTC-2024-036 / INTC-P-704
09/04/2024

Abstract: We propose to utilise the facilities available at ISOLDE to perform an offline implantation of 200 kBq of ^{226}Ra into a glassy carbon backing target to be used for a measurement of its nuclear charge radius by means of muonic atom spectroscopy. Such a measurement is crucial for any future measurement of atomic parity violation using radium and provides an important absolute benchmark for laser spectroscopy.

Summary of requested shifts: 6 shifts (split into 1 run over 1 year) with no proton irradiation

1 Introduction

Next to its mass the charge radius of a nucleus is one of its defining properties and thus fundamental for understanding and calculating its interactions. While charge radii have been measured and studied since a long time there is still room for surprises as the recent measurements with muonic hydrogen [1], [2], that lead to the proton radius puzzle [3], showed.
As an example, where precise knowledge of the charge radius is lacking, serves the potential measurement of atomic parity violation (APV) in a single Ra^+ ion [4]–[6]. The parity violating signals arise through the weak interaction between the nucleus and its surrounding lepton cloud. A precise measurement of atomic parity violation has so far only been achieved in the case of cesium through measurements of the $6s - 7s$ transition amplitudes [7]. In the end such a measurement allows to extract the weak mixing angle – the Weinberg angle θ_W – complementary to its extractions from electron scattering, neutrino scattering or at a high-energy collider. Together they allow to probe the running of $\sin^2\theta_W$ as a function of momentum transfer as predicted by the Standard Model. However, in order to extract θ_W from the transition amplitudes the interaction of the nucleus with the corresponding electrons has to be calculated with precision. In the case of radium this means knowledge of its charge radius at a level of at least 0.2% [8], [9].
The study of the charge radius of radium has a long history at ISOLDE. From the original laser spectroscopy work with collinear fluorescence spectroscopy to the more recent work with collinear resonance ionization spectroscopy, the changes in the charge radius from ^{208}Ra to ^{233}Ra have been investigated [10], [11]. More recently, the study of RaF molecules with collinear resonance ionization spectroscopy has also sparked new interest in isotope shifts of radium and the determination of changes in the charge radius [12]–[14]. However, the impact of these measurements are still limited as relative changes until an absolute charge radius can be determined with which to anchor the whole isotopic chain [15].

2 The muX experiment

Muonic atom spectroscopy is traditionally the method of choice for the measurement of absolute charge radii. In muonic atom spectroscopy a negative muon beam is stopped in a target made of the desired material. After slowing down, the muon is captured by the nucleus and cascades down from a high initial state around $n \approx 14$ to the ground state. While the cascade initially occurs mainly through Auger transitions the lower states are passed through radiative transitions. By measuring the emitted x-ray photons (which for high-Z muonic atoms can reach up to 10 MeV) the binding energies of the various levels of the muonic atom can be mapped out. Comparing the measured energy levels with calculations taking the finite size of the nucleus into account allows to extract its charge radius. While in principle a single transition energy is sufficient to extract the charge radius, in practice a multitude of transitions is analyzed to constrain the calculations and to determine additional nuclear effects such as nuclear polarization from the data itself. An impressive precision on the charge radius can be achieved amounting in the case of ^{208}Pb to 0.02% [16]. The correct treatment of all relevant effects [17] (QED corrections,

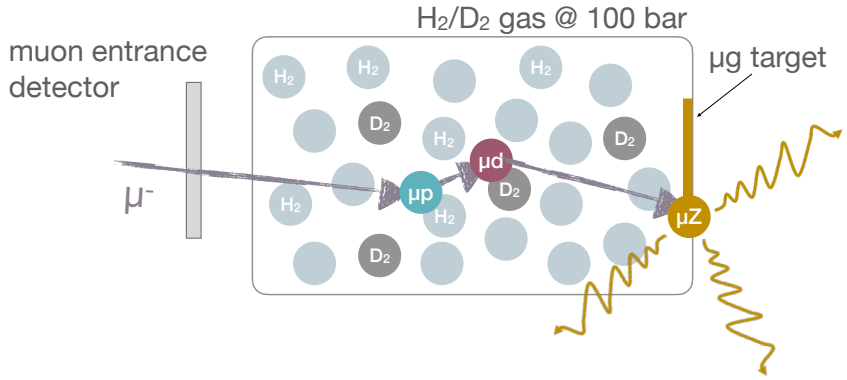

Figure 1: Sketch and short description of the method employed to measure muonic x rays emitted from a target with only microgram mass. The negative muon enters a 100 bar hydrogen gas cell with a small admixture of deuterium. Upon stopping, the muon forms muonic hydrogen μp and transfers to a deuteron upon collision with a deuterium molecule forming muonic deuterium μd. Due to its low scattering cross section, μd can travel over a large distance potentially reaching the microgram target at the back of the cell. Here, the muon transfers again to the target nucleus thereby emitting the characteristic muonic x rays.

nuclear polarization, deformation, nuclear excitations, ...) in the analysis of the muonic spectra is challenging and usually by far limits the precision that can be achieved.
As a standard negative muon beam cannot be stopped in the small quantities typically available for highly radioactive elements such as ^{226}Ra, the muX collaboration has over the last years developed a new method that is capable of performing muonic atom spectroscopy on samples available in microgram quantities [18]. The method relies on transfer reactions taking place inside a high-pressure hydrogen gas cell operating at 100 bar, corresponding to about 10% of liquid hydrogen density, with a small admixture of deuterium. The method is inspired by the work described in Refs. [19]–[21] and the wealth of knowledge gained in the pursuit of muon catalyzed fusion (see, e.g., Refs. [22], [23]) on the behavior and interaction of the muonic hydrogen isotopes inside gas cells. A sketch and a very brief description of the method can be found in Fig. 1. The gas cell is then surrounded by an array of germanium detectors to efficiently and precisely measure the emitted x rays from the target.
While the method described above was validated with thin gold targets with masses down to 5 μg, measurements of radioactive elements have since successfully been completed. Figure 2 shows the spectrum measured for ^{248}Cm with the MiniBall detector array during the CERN Long Shutdown 2 and the statistical precision on the charge radius and quadrupole moment that can be achieved from such a measurement. The final precision achievable will be limited by the systematic uncertainties and here especially from the calculation of corrections that need to be applied.
The 15 μg ^{248}Cm target was prepared by a combination of molecular plating [24] and drop-on-demand [25] on a glassy carbon backing. While the measurement was in the end successful, several issues were observed that limited the performance of the target: i) the target was contaminated with palladium from the molecular plating process, ii) in

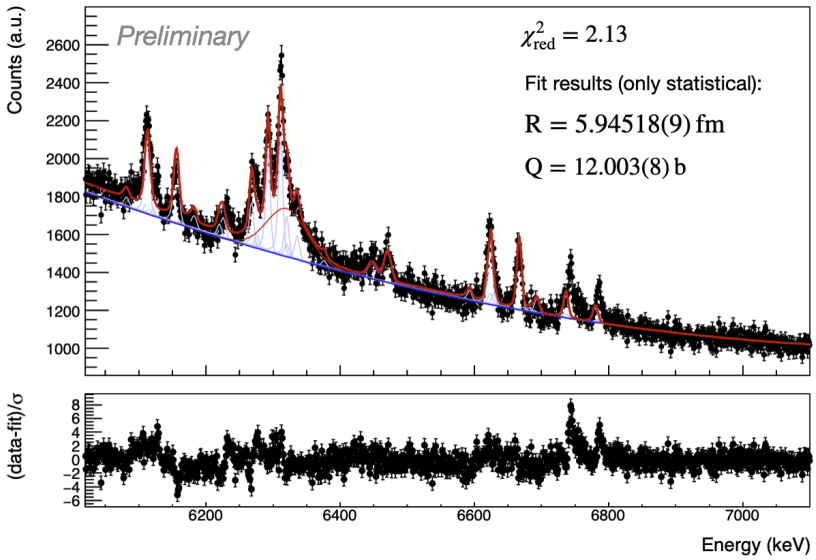

Figure 2: X-ray spectrum of the $2p-1s$ transitions in muonic ^{248}Cm together with the fit extracting the nuclear charge radius R and the quadrupole moment Q. The systematic uncertainty will in the end dominate the uncertainty on the two parameters.

addition to ^{248}Cm a small amount of ^{246}Cm is present as well, and iii) the element of choice is deposited in molecular form. All of these three effects lead to a reduction of the overall efficiency as the μd atoms that reach the target can transfer to these other elements thereby reducing the amount of good, target x rays that can be measured. In addition to ^{248}Cm, several attempts were already made to measure ^{226}Ra using targets prepared by both molecular plating and drop-on-demand. While the latest target prepared by molecular plating showed promise and the very first hints of muonic ^{226}Ra x rays were observed, its efficiency was not enough to perform a measurement with good statistical precision.

In order to circumvent some of the drawbacks of the two target production methods described above, the muX collaboration has started to develop methods in order to use implanted targets [26]. This of course allows to use mass separation available for ion beams and to implant the target element in its atomic form into a suitable backing material. As a first step, targets were prepared that featured a thin, sputtered gold layer covered on top by a sputtered graphite layer of variable thickness. Figure 3 shows the results of these measurements. While the muon capture rate on gold of course drops with increasing graphite thickness, still a sizeable amount of μd atoms penetrate through graphite layers of several tens of nanometers. With these first results in hand, tests and measurements were subsequently successfully performed with gold implantations at 4.5, 27 and 90 keV. In addition, a first implanted, radioactive target was measured just last year - 7.5 μg of ^{40}K (equivalent to 1.1×10^{17} atoms) implanted at an energy of 30 keV.

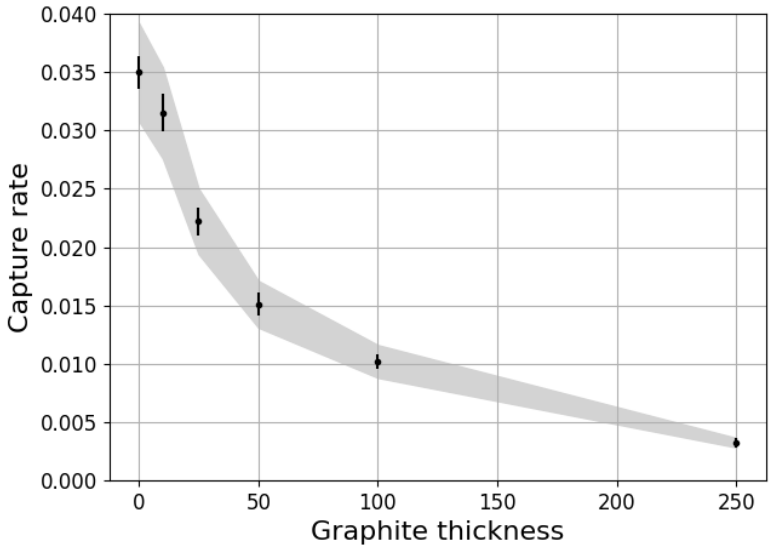

Figure 3: Attenuation of the muon capture rate on gold as a function of the graphite thickness in nanometers covering the gold layer. [26]

3 Implantation of ^{226}Ra

Based on the successful developments described in the previous section, we propose to use the capabilities and facilities of ISOLDE at CERN, in order to prepare an implanted ^{226}Ra target to be used in the muX experiment at PSI. The envisaged target mass is 5.5 μg, which corresponds to 100 times the approval limit (LA) or 200 kBq. The total amount of ^{226}Ra atoms is 1.46×10^{16}. This amount of target material is the maximum allowed in the experimental hall of PSI and necessary in order to ensure a good statistics measurement.

The proposed implantation scheme outlined below is based on our recent separation of ^{110m}Ag at ISOLDE [27] and the experience of the MEDICIS team with ^{224}Ra [28], where an efficiency of 40% for surface ionisation was observed. Enhancement of the ionisation efficiency through laser ionisation is known [29], as well as the use of molecular beams [12], but for simplicity we propose to use surface ionisation alone and base our further estimations on that. We will employ the GPS separator of ISOLDE offline and load it with commercially purchased ^{226}Ra solutions. The carrier free ^{226}Ra solution will consist of radium nitrate dissolved in 1 M HNO_3. The collection will be done at the GLM or GHM station. The extracted particle current at 30 keV will be restricted to stay below the ion load limit expected to be around 20 to 130 nA. As we plan to produce two implanted targets, we propose to perform the first implantation at 20 nA followed by the second implantation at 100 nA. The relevant parameters for the implantation and the calculation of the total duration are given in Table 1. The total duration for the implantation is 39 hours for the two targets. Including time for preparation and target change **we thus request 6 shifts**.

The backing material for the implantation is a glassy carbon disk (SIGRADUR K) with a

Table 1: Relevant parameters for the offline implantation of 1.46×10^{16} radium atoms into the backing material equivalent to 650 nAh. We foresee the production of two targets using two different maximum ion currents.

initial activity	ionisation efficiency	ion current	implantation duration
500 kBq	40%	20 nA	32.5 h
500 kBq	40%	100 nA	6.5 h

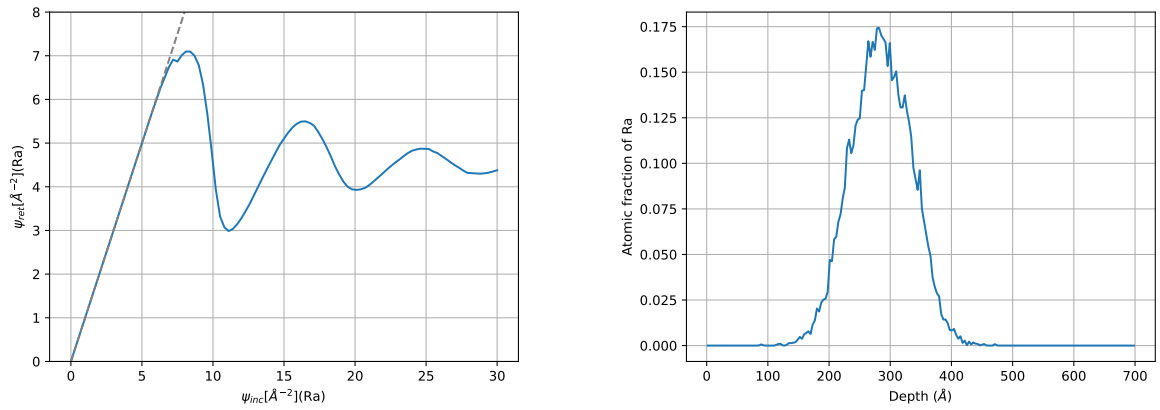

Figure 4: (Left) TRIDYN simulation for the dependence of the retained fluence (y-axis) versus incoming fluence (x-axis). At an incoming fluence of 7.5 $Å^{-2}$ self-sputtering effects start to play a signifcant role. (Right) Simulated implantation depth profile for the 1.46×10^{16} radium ions in the glassy carbon backing disk.

thickness of 1 mm and a diameter of 16 mm [27]. The implantation is ideally distributed over the central 10 mm diameter area matching well the expected beam width of 8 mm and with potentially utilising the existing rastering capabilities of the beamline. We have performed TRIDYN [30] implantation simulations using the parameters above in order to assess the implantation depth and self-sputtering limits. These simulations have also been performed for our previous implantations and proved to be reasonably reliable [31]. Figure 4 shows the results of these simulations. The plot on the left shows the relation between the retained fluence versus the incoming fluence. Beyond a fluence of around 7.5 $Å^{-2}$ self-sputtering effects start to play a role and the retained fluence drops. The expected 1.46×10^{16} atoms distributed over a 10 mm diameter area leads to a fluence of 1.9 $Å^{-2}$ - therefore well below any critical limits. Additionally, the depth profile shown on the right predicts an implantation depth of around 30 nm, which should result in only a small attenuation of the signal as shown in Fig. 3. We have also looked at recoil-sputtering effects after the implantation due to decays using SRIM/TRIM [32] simulations, but found only a small expected loss due to these effects [31].
The amount of implanted radium ions will be monitored through the measured ion current and γ-ray spectroscopy. The 186 keV γ ray emitted in the decay of ^{226}Ra with a branching of 3.64% offers direct monitoring of the radium activity present in the sample. While a liquid nitrogen cooled high-purity germanium is in principle the detector of choice for

such a measurement, other options are available in case of safety concerns due to the use of liquid nitrogen in this environment. These options are the use of an electrically cooled high-purity germanium detector or of inorganic scintillators such as cerium or lanthanum bromide.
It is clear that the amount of ^{226}Ra to be used is significant and we are aware of the associated safety concerns. We have already contacted relevant personnel at CERN in order to follow all required protocols and procedures in order to conduct the implantation in a safe way and limit contamination to a minimum.
After implantation, the targets will be stored under vacuum in order to reduce any degradation of the targets due to contact with air and avoid potential molecular formation, as well as to avoid the uncontrolled release of ^{222}Rn gas. Subsequently, the targets will be shipped to PSI where they are transferred to the muX target chambers and used for muonic atom spectroscopy in the following muon beam period depending on approval and scheduling at PSI.

4 Summary of beam time request

In order to collect two samples of ^{226}Ra with 1.46×10^{16} atoms, we request **6 shifts of beam time without protons**, as described in Table 1.

References

[1] R. Pohl *et al.*, "The size of the proton," *Nature*, vol. 466, p. 213, 2010. DOI: 10.1038/nature09250.

[2] A. Antognini *et al.*, "Proton Structure from the Measurement of 2S-2P Transition Frequencies of Muonic Hydrogen," *Science*, vol. 339, p. 417, 2013. DOI: 10.1126/science.1230016.

[3] R. Pohl *et al.*, "Muonic Hydrogen and the Proton Radius Puzzle," *Annual Review of Nuclear and Particle Science*, vol. 63, p. 175, 2013. DOI: 10.1146/annurev-nucl-102212-170627.

[4] L. W. Wansbeek *et al.*, "Atomic parity nonconservation in Ra^+," *Phys. Rev. A*, vol. 78, 050501(R), 2008. DOI: 10.1103/PhysRevA.78.050501.

[5] O. O. Versolato *et al.*, "Laser spectroscopy of trapped short-lived Ra^+ ions," *Phys. Rev. A*, vol. 82, p. 010 501, 2010. DOI: 10.1103/PhysRevA.82.010501.

[6] M. Nuñez Portela *et al.*, "Ra^+ ion trapping: toward an atomic parity violation measurement and an optical clock," *Applied Physics B*, vol. 114, p. 173, 2014. DOI: 10.1007/s00340-013-5603-2.

[7] C. S. Wood *et al.*, "Measurement of Parity Nonconservation and an Anapole Moment in Cesium," *Science*, vol. 275, p. 1759, 1997. DOI: 10.1126/science.275.5307.1759.

[8] K. P. Jungmann, "Muon physics possibilities at a muon-neutrino factory," *Hyperfine Interactions*, vol. 138, p. 463, 2001. DOI: 10.1023/A:1020826729142.

[9] O. O. Versolato *et al.*, private communication, 2015.

[10] K. Wendt, S. A. Ahmad, W. Klempt, *et al.*, "On the hyperfine structure and isotope shift of radium," *Z. Phys. D*, vol. 4, pp. 227–241, 1987. DOI: 10.1007/BF01436633.

[11] K. M. Lynch *et al.*, "Laser-spectroscopy studies of the nuclear structure of neutron-rich raidum," *Phys. Rev. C*, vol. 97, p. 024 309, 2018. DOI: 10.1103/PhysRevC.97.024309.

[12] R. F. Garcia Ruiz *et al.*, "Spectroscopy of short-lived radioactive molecules," *Nature*, vol. 581, pp. 396–400, 2020. DOI: 10.1038/s41586-020-2299-4.

[13] S. M. Udrescu *et al.*, "Isotope shifts of radium monofluoride molecules," *Phys. Rev. Lett*, vol. 127, p. 033 001, 2021. DOI: 10.1103/PhysRevLett.127.033001.

[14] M. Athanasakis-Kaklamanakis, S. G. Wilkins, A. A. Breier, *et al.*, "King-plot analysis of isotope shifts in simple diatomic molecules," *Phys. Rev. X*, vol. 13, p. 011 015, 2023. DOI: 10.1103/PhysRevX.13.011015.

[15] T. E. Cocolios, "A new perspective on charge radii around Z=82," *Hyperfine Interact.*, vol. 238, p. 16, 2017. DOI: 10.1007/s10751-016-1391-5.

[16] P. Bergem *et al.*, "Nuclear polarization and charge moments of ^{208}Pb from muonic x rays," *Phys. Rev. C*, vol. 37, p. 2821, 1988. DOI: 10.1103/PhysRevC.37.2821.

[17] E. Borie and G. A. Rinker, "The energy levels of muonic atoms," *Rev. Mod. Phys.*, vol. 54, p. 67, 1982. DOI: 10.1103/RevModPhys.54.67.

[18] A. Adamczak *et al.*, "Muonic atom spectroscopy with microgram target material," *Eur. Phys. J. A*, vol. 59, no. 2, p. 15, 2023. DOI: 10.1140/epja/s10050-023-00930-y. arXiv: 2209.14365 [nucl-ex].

[19] J. Kraiman *et al.*, "Diffusion of Muonic Deuterium in D_2 Gas," *Phys. Rev. Lett.*, vol. 63, p. 1942, 1989. DOI: 10.1103/PhysRevLett.63.1942.

[20] P. Strasser, K. Nagamine, T. Matsuzaki, *et al.*, "Muonic Atoms of Unstable Nuclei," *AIP Conf. Proc.*, vol. 793, no. 1, Y. Yamazaki and M. Wada, Eds., pp. 242–257, 2005. DOI: 10.1063/1.2121987.

[21] P. Strasser *et al.*, "Muon spectroscopy with trace alkaline-earth and rare-earth isotopes implanted in solid D_2," *Hyperfine Interact.*, vol. 193, p. 121, 2009. DOI: 10.1007/s10751-009-0055-0.

[22] L. I. Ponomarev, "Muon catalysed fusion," *Contemporary Physics*, vol. 31, p. 219, 1990. DOI: 10.1080/00107519008222019.

[23] C. Petitjean, "The μCF Experiments at PSI –A Conclusive Review," *Hyperfine Interactions*, vol. 138, no. 1, p. 191, 2001. DOI: 10.1023/A:1020883708302.

[24] W. Parker and R. Falk, "Molecular plating: A method for the electrolytic formation of thin inorganic films," *Nucl. Instr. Meth.*, vol. 16, p. 355, 1962. DOI: 10.1016/0029-554X(62)90142-8.

[25] R. Haas *et al.*, "Development and characterization of a Drop-on-Demand inkjet printing system for nuclear target fabrication," *Nucl. Instrum. Meth. A*, vol. 874, pp. 43–49, 2017. DOI: 10.1016/j.nima.2017.08.027.

[26] M. Heines *et al.*, "Muonic x-ray spectroscopy on implanted targets," *Nucl. Instrum. Meth. Phys. B*, vol. 541, pp. 173–175, 2023. DOI: 10.1016/j.nimb.2023.05.036.

[27] M. Deseyn *et al.*, *110mAg collection report (IS672)*, Mar. 2024. DOI: 10.5281/zenodo.10794181.

[28] C. Duchemin, *Medicis operation in 2023*, https://indico.cern.ch/event/1351618, 2023.

[29] T. o. Day Goodacre, "Radium ionization scheme development: The first observed autionizing states and optical pumping effects in the hot cavity environment," *Spectrochimica Acta B*, vol. 150, pp. 99–104, 2018. DOI: 10.1016/j.sab.2018.10.002.

[30] W. Möller and W. Eckstein, "Tridyn—a TRIM simulation code including dynamic composition changes," *Nuclear Instruments and Methods in Physics Research Section B: Beam Interactions with Materials and Atoms*, vol. 2, no. 1-3, pp. 814–818, 1984. DOI: 10.1016/0168-583X(84)90321-5.

[31] M. Deseyn, *Maximizing the radionuclide collection efficiency at CERN-MEDICIS: A case study on terbium collections and sputtering*, CERN-THESIS-2023-111, 2023.

[32] J. F. Ziegler, M. D. Ziegler, and J. P. Biersack, "SRIM–the stopping and range of ions in matter (2010)," *Nuclear Instruments and Methods in Physics Research Section B: Beam Interactions with Materials and Atoms*, vol. 268, no. 11-12, pp. 1818–1823, 2010. DOI: 10.1016/j.nimb.2010.02.091.

5 Details for the Technical Advisory Committee

5.1 General information

Describe the setup which will be used for the measurement. If necessary, copy the list for each setup used.

☒ Permanent ISOLDE setup: GLM collection chamber

- ☒ To be used without any modification
- ☐ To be modified: *Short description of required modifications.*

☐ Travelling setup (*Contact the ISOLDE physics coordinator with details.*)

- ☐ Existing setup, used previously at ISOLDE: *Specify name and IS-number(s)*
- ☐ Existing setup, not yet used at ISOLDE: *Short description*
- ☐ New setup: *Short description*

5.2 Beam production

For any inquiries related to this matter, reach out to the target team and/or RILIS (please do not wait until the last minute!). For Letters of Intent focusing on element (or isotope) specific beam development, this section can be filled in more loosely.

- Requested beams:

Isotope	Production yield in focal point of the separator ($/\mu$C)	Minimum required rate at experiment (pps)	$t_{1/2}$
^{226}Ra	Not applicable	100 nA	1600 years

- Full reference of yield information: external sample provided by the Users and loaded according to the protocol developed for MEDICIS.
- Target - ion source combination: External sample + surface ion source + small mass marker for beam tuning
- RILIS: May be set for Ra but not necessary
  - ☐ Special requirements: no
- Additional features?
  - ☐ Neutron converter: not applicable
  - ☐ Other: no
- Expected contaminants: none
- Acceptable level of contaminants: not applicable

- Can the experiment accept molecular beams? no: other element may reduce the muon capture during the muonic x-ray spectroscopy experiment.
- Are there any potential synergies (same element/isotope) with other proposals and LOIs that you are aware of? Yes: IS725

5.3 HIE-ISOLDE

Not applicable

5.4 Shift breakdown

The beam request only includes the shifts requiring radioactive beam, but, for practical purposes, an overview of all the shifts is requested here. Don't forget to include:

- Isotopes/isomers for which the yield need to be determined
- Shifts requiring stable beam (indicate which isotopes, if important) for setup, calibration, etc. Also include if stable beam from the REX-EBIS is required.

An example can be found below, please adapt to your needs. Copy the table if the beam time request is split over several runs.

Summary of requested shifts:

With protons	Requested shifts
not applicable	
Without protons	Requested shifts
Stable beam tuning from mass marker	1
Low-intensity collection	4
Sample exchange	0.5
High-intensity collection	1
Sample retrieval	0.5

5.5 Health, Safety and Environmental aspects

5.5.1 Radiation Protection

- If radioactive sources are required:
  - Purpose? Calibrating the γ-ray detector
  - Isotopic composition? Typical sources available at ISOLDE (^{133}Ba, ^{137}Cs, ^{152}Eu, ...)
  - Activity? Using the sources already available at ISOLDE
  - Sealed/unsealed? Sealed
- For collections:
  - Number of samples? 2
  - Activity/atoms implanted per sample? 1.46×10^{16} atoms, corresponding to 200 kBq, or 100 LA
  - Post-collection activities? on-site characterization with γ-ray and α-decay spectroscopy; storage under vacuum; shipping to PSI to perform muonic x-ray spectroscopy.

5.5.2 Only for traveling setups

not applicable